EPR and ^{14}N electron-nuclear double-resonance measurements on the ionized nearest-neighbor dinitrogen center in diamond

O. D. Tucker, M. E. Newton,* and J. M. Baker
Department of Physics, University of Oxford, Clarendon Laboratory, Parks Road, Oxford, OX1 3PU, United Kingdom
(Received 6 June 1994)

The nearest-neighbor substitutional nitrogen center $[N\text{-}N]^0$ (*A* center), is one of the most common defects in natural diamond. $[N\text{-}N]^0$ is diamagnetic and therefore cannot be studied by electron paramagnetic resonance (EPR). However, the $[N\text{-}N]^+$ center is paramagnetic, and we report detailed EPR and electron-nuclear double-resonance (ENDOR) studies on this center. The ^{14}N and ^{13}C hyperfine coupling matrices show that approximately 100% of the unpaired electron population is in the lowest-energy antibonding orbital formed between the two nitrogen atoms, which are equivalent. Using orthogonality and simple geometric considerations the ^{14}N hyperfine interaction is used to make an estimate of the length of the N-N bond in the $[N\text{-}N]^+$ center. The result appears consistent with more sophisticated calculations on the $[N\text{-}N]^0$, and single substitutional nitrogen centers $[N\text{-}C]^0$. For several defects incorporating substitutional ^{14}N (including $[N\text{-}N]^+$) the quadrupole interaction is proportional to the fraction of unpaired electron population on the nitrogen atom. A simple molecular orbital calculation explains this finding, and determines that the quadrupole interaction for a single unpaired electron in a $2p$ orbital on ^{14}N is $-6.7(3)$ MHz. $[N\text{-}N]^+$ can be created in some natural diamonds by illumination with photons of energy greater than 3.0 eV. Studies on the number of $[N\text{-}N]^+$ centers remaining after the optical excitation is switched off indicate that there is a wide distribution of lifetimes, presumably resulting from a large variation in the separation between a $[N\text{-}N]^+$ center and its electron trap and/or donor. Below about 25 K, the decay rate is independent of temperature, indicating tunnelling between the donor and/or trap and the $[N\text{-}N]^+$ center; at higher temperatures thermally activated hopping also contributes. In powered diamond $[N\text{-}N]^+$ can be observed without illumination whereas in the single crystal it was only observed after illumination, suggesting that a defect created near the surface could be acting as a trap and/or donor. It appears that $[N\text{-}N]^+$ can be created via electron capture by $[N\text{-}N]^{2+}$ or by ionization of $[N\text{-}N]^0$, or possibly both, depending on the traps and donors available.

I. INTRODUCTION

A. Nitrogen in diamond

Most synthetic diamonds grown at high temperatures and pressures contain paramagnetic single substitutional nitrogen atoms ($[N\text{-}C]^0$) often referred to as *P*1 centers.[1,2] The $[N\text{-}C]^0$ concentration can be as high as 500 parts nitrogen per million carbon atoms (ppm). Diamond grown by chemical-vapor deposition also often contains $[N\text{-}C]^0$ centers: indeed concentrations as high as 300 ppm have been measured in flame-grown diamond.[3] Diamonds containing nitrogen predominately in the form of single-atom substitutional impurities are referred to as type Ib. The notation $[X\text{-}Y]^q$ is used for substitutional defects, where X or Y refer to nitrogen or carbon atoms, and q indicates the charge state of the cluster. For the single substitutional nitrogen center, approximately 24% of the unpaired electron population is on the nitrogen and 67% on one carbon neighbor.[1,2] It is this unique carbon neighbor which is indicated in the notation $[N\text{-}C]^0$.

Nitrogen is the major impurity in most natural diamonds; concentrations of several thousand ppm are not uncommon. The majority of the nitrogen is incorporated in aggregates rather than in $[N\text{-}C]^0$ centers, and these diamonds are classified as type Ia. Two different dominant forms of aggregates have been recognized: The *A* and *B* centers. Diamonds containing predominately *A* or *B* centers are referred to as type Ia*A* and Ia*B*, respectively.

The aggregation of $[N\text{-}C]^0$ centers to form *A* centers has been studied by many workers.[4–7] When thermally annealing type Ib synthetic diamonds, it has been shown that the rate of formation of *A* centers is proportional to the square of the initial concentration of single substitutional nitrogen atoms, showing that the *A* center involves two nitrogen atoms.[6] It is now accepted that the *A* center consists of a pair of adjacent substitutional atoms, $[N\text{-}N]^0$, and this is the notation used herein to represent this center. The model was proposed by Davies,[8] who made uniaxial stress measurements on an optical-absorption line at 3.8 eV, which showed that the defect has trigonal symmetry. $[N\text{-}N]^0$ centers give rise to infrared absorption at 1282, 1203, 1093, and 480 cm^{-1}.[9] Recent *ab initio* calculations by Briddon and Jones[10] have shown that the $[N\text{-}N]^0$ model satisfactorily explains these infrared absorptions, and give a doubly occupied level around midgap, accounting for the 3.8 eV absorption edge seen in type Ia *A* diamonds.

Evans and Qi[6] have shown that the *B* centers can be produced by annealing type Ia *A* diamond. However the reaction kinetics are not well understood, and the structure of the *B* center has not been unambiguously deter-

mined. The current consensus is that the *B* center probably consists of four nitrogens around a vacancy, as proposed by Loubser and van Wyk (unpublished). Neither the *A* or *B* centers are paramagnetic.

B. Previous measurements on the $[N\text{-}N]^+$ center

Vay Wyk and Loubser[11] observed electron paramagnetic resonance (EPR) from a dinitrogen center in gem-quality Cape Yellow diamonds while illuminating with ultraviolet light. Their analysis showed that an unpaired electron is in an orbital on two equivalent neighboring substitutional nitrogen atoms. They suggested that this center is a derivative of the diamagnetic $[N\text{-}N]^0$ center, and labeled it *W*24. We use the more informative notation $[N\text{-}N]^+$, since the measurements presented here confirm this model. Other features they observed are as follows:

(1) The $[N\text{-}N]^+$ center was not observed in the type Ia*B* diamonds studied.

(2) The concentration of $[N\text{-}N]^+$ centers created by illumination is not simply proportional to the concentration of $[N\text{-}N]^0$ centers.

(3) The concentration of $[N\text{-}N]^+$ created by illumination is larger in diamonds showing strong *N*3-center luminescence. (The *N*3 optical center is the *P*2 EPR center,[12] which is known to consist of three substitutional nitrogen atoms around a vacancy. It is not the EPR center elsewhere labeled *N*3.[13] To avoid confusion we use the notation $[N_3V]^0$ for the *N*3(optical) alias *P*2(EPR) center.)

(4) In the majority of diamonds studied, a high concentration of $[N\text{-}N]^+$ centers was created by illumination only when the concentration of $[N_3V]^0$ centers was more than 30 times that of $[N\text{-}C]^0$.

(5) Light of wavelength shorter than 415(5) nm (3.0 eV) is required to produce $[N\text{-}N]^+$.

(6) $[N\text{-}N]^+$ is not generated uniformly throughout the diamond.

(7) The lifetime of $[N\text{-}N]^+$ after switching off the illumination is sample dependent.

II. EXPERIMENTAL

A. Samples

Three diamonds that showed strong *N*3 ($[N_3V]^0$) luminescence when excited with 366 nm radiation were selected for study from a collection of natural Cape Yellow diamonds. The samples were cut and polished into cubes, with faces approximately parallel to crystallographic planes {100} or {110}. In all three diamonds, $[N\text{-}N]^+$ centers were observed by EPR when illuminating with light of wavelength shorter than 415 nm. EPR measurements showed that the concentrations of $[N\text{-}C]^0$, $[N_3V]^0$, and $[N\text{-}N]^+$ centers were very similar in all three specimens. We report on measurements from only one of the three samples, since all gave essentially the same results.

B. Spectrometer used for EPR and electron-nuclear double-resonance (ENDOR) measurements

EPR measurements were made at temperatures between 3.7 and 300 K, using a Bruker TE_{104} resonant cavity operating at about 9.65 GHz, in conjunction with an Oxford Instruments ESR900 continuous-flow cryostat. Measurements of the electronic *g* values were made by comparison with the $[N\text{-}C]^0$ center. The $[N\text{-}C]^0$ center has an isotropic *g* value of 2.0024(1),[1] which is temperature independent between 3.7 and 300 K. Continuous-wave ENDOR measurements were made at approximately 9.65 GHz using a TM_{110} cavity constructed in the Clarendon Laboratory and described previously.[14]

C. Arrangements for optical excitation

For the studies presented in this paper, EPR and ENDOR measurements were made at temperatures down to 3.7 K, while illuminating the sample with ultraviolet (uv) light. The light source was a 100-W mercury arc lamp. The light was guided to the top of the cryostat by a uv(*A*)/blue liquid light guide, where it was directed onto the end of a circular quartz rod inserted into a cryostat cold finger, which had the sample mounted on the other end. The sample could therefore be illuminated in the ENDOR/EPR cavity, and held at any desired temperature between 3.7 and 300 K. Measurements with a light meter (Photon Control Model 11) showed that a maximum of 200 mW of available light power was incident on the sample. To study the spectral response of the specimen under investigation, we used a high-throughput $\frac{1}{4}$-m monochromator (300–600 nm), with an 8 nm bandpass. When using the monochromator, the incident light power on the sample was less than 2 mW. For studies of the lifetime of the $[N\text{-}N]^+$ center, a computer controlled electronic shutter (Melles Griot) was used to switch the light on and off.

III. RESULTS

A. Concentrations of the $[N\text{-}N]^+$, $[N\text{-}C]^0$, and $[N_3V]^0$ centers

The diamond studied contained the $[N\text{-}N]^+$, $[N\text{-}C]^0$, $[N_3V]^0$, and *W*21 centers. The *W*21 center, first observed by Loubser, van Wyk, and Welbourn,[15] is thought to involve three nitrogen atoms in adjacent substitutional sites. Comparison with a calibrated reference sample indicated that the absolute concentrations on the $[N\text{-}N]^+$, $[N\text{-}C]^0$, and $[N_3V]^0$ centers were 1, 4.5, and 190 ppm, respectively, with uncertainties of about 20%. That of the *W*21 was too low to allow accurate measurement. Great care was taken to allow for the effects of power saturation, which is considered in greater detail in Sec. III B.

B. EPR saturation effects

Absolute and comparative EPR absorption measurements of the $[N\text{-}N]^+$, $[N\text{-}C]^0$, and $[N_3V]^0$ centers are difficult because of saturation and cross-relaxation effects. It became clear that at helium temperatures the average

lifetime of the $[N\text{-}N]^+$ centers created by illumination is very long indeed, and that illumination has a secondary effect of effectively desaturating the $[N\text{-}N]^+$, $[N\text{-}C]^0$, and $[N_3V]^0$ EPR signals. There are two possible reasons, firstly the light causes heating of the diamond, reducing saturation, and secondly it creates the possibility of rapid saturation transfer via electrons temporarily excited to the conduction band, as has been observed during studies in silicon.[16] The enhancement technique described by Newton and Baker[17] (achieved by sweeping rf excitation rapidly and repeatedly through the ENDOR transitions) was used to improve the EPR and ENDOR signal-to-noise ratios. The light and the rf desaturate the EPR via different pathways, and their effects are additive.

C. EPR measurements of ^{15}N and ^{13}C hyperfine structure

^{15}N has a natural abundance of 0.366% so that, in the $[N\text{-}N]^+$ center, the probability of having one ^{14}N and one ^{15}N is 0.73%, both ^{14}N is 99.27%, or both ^{15}N is 0.001%. The positions of EPR transitions from ^{14}N-^{15}N pairs can be accurately estimated because the ^{14}N hyperfine parameters, electronic g value and ratio of nuclear g factors are known. Figure 1 shows an experimental EPR spectrum and a simulation thereof; clearly the lines from ^{14}N-^{15}N pairs are well reproduced. This provides independent confirmation that the $[N\text{-}N]^+$ center incorporates two nitrogen atoms.

One expects to observe further weak transitions due to the coupling between the unpaired electron and the ^{13}C nuclei around the nitrogen atoms of the $[N\text{-}N]^+$ center. The sets of equivalent neighboring carbon atom sites are shown shaded in Fig. 2. There are six nearest-neighbor carbon sites (light shading), and two groups of more distant equivalent neighbors containing six (medium shading) and 12 members (dark shading). The natural abundance of ^{13}C is 1.1%, and hence the probability that one of a group of six equivalent neighbors is a ^{13}C is 0.066, and that one of the group of 12 equivalent neighbors is a ^{13}C atom is 0.132. Therefore, for an isotropic ^{13}C hyperfine interaction, we expect satellites around the main $[N\text{-}N]^+$ lines with $\frac{1}{30}$th (six equivalent neighbors), or $\frac{1}{15}$th (12 equivalent neighbors) of the intensity of the primary lines they flank.

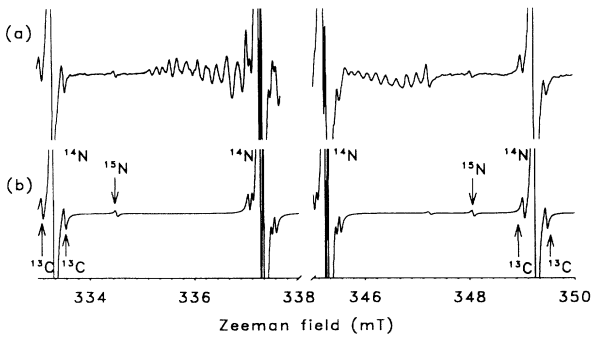

FIG. 1. 9.65-GHz EPR spectra: (a) Experimental spectrum, $B\|\langle 100\rangle$ and $T=5$ K at (b) simulated $[N\text{-}N]^+$ spectrum, $B\|\langle 100\rangle$, including ^{14}N, ^{15}N, and ^{13}C lines.

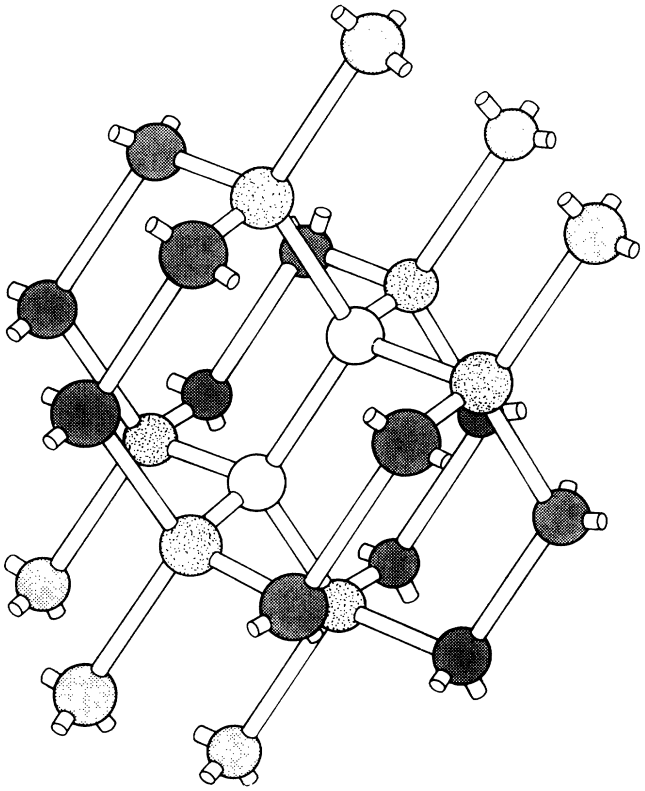

FIG. 2. $[N\text{-}N]^+$ defect in diamond lattice. The two nitrogen atoms are shown unshaded, and the various groups of carbon neighbors are distinguishable by their shading. See text for further details.

The ^{13}C satellites flanking the $[N\text{-}N]^+$ ^{14}N hyperfine EPR lines can be clearly seen in Fig. 1(a). The simulation in Fig. 1(b) is produced by assuming six equivalent neighbors, Lorentzian line shape, and a linewidth (halfwidth at half height) of 0.042(2) mT; it clearly reproduces the experimental details accurately. For all orientations of the applied Zeeman field only one set of ^{13}C satellites were observed around the main $[N\text{-}N]^+$ lines. To within the accuracy of our measurements the separation, 0.44(2) mT, of the satellites was found to be independent of the orientation of the magnetic field, and they were always centered about the main ^{14}N hyperfine lines.

D. Infrared and uv/visible optical-absorption measurements

Infrared and uv/visible absorption were measured using a Perkin-Elmer 1710 infrared Fourier-transform spectrometer and a Perkin-Elmer Lambda-9 spectrophotometer, respectively. The infrared absorption in the one-phonon region is shown in Fig. 3. Simulation of this spectrum using only a combination of the infrared absorption spectra from the $[N\text{-}C]^0$, A, and B centers (A and B components) does not satisfactorily reproduce the experimental data. However, inclusion of the D component,[18,19] which is attributed to platelet stimulated lattice vibrational modes, improves the simulation. Using the parameters determined by Woods and coworkers,[20,21] the concentrations on the $[N\text{-}N]^0$ and B

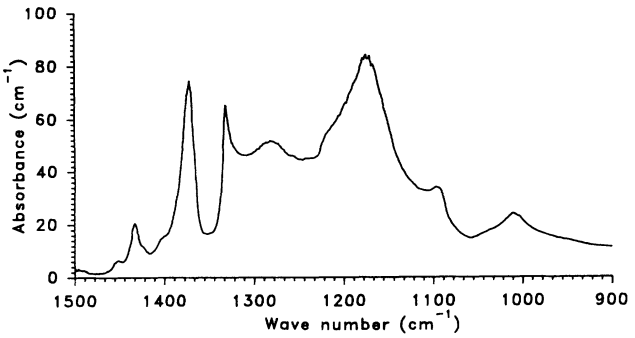

FIG. 3. Infrared absorption spectrum of the diamond studied, measured at 298 K with a resolution of 1 cm^{-1}.

centers were estimated at 150 and 750 ppm, respectively (assuming four nitrogen atoms per B center). There is clearly a strong platelet peak (B') at 1370 cm^{-1} and additional structure near 1426 cm^{-1}.[19]

Following the notation usually adopted[19] for infrared characterization of diamonds, the specimen studied here can be characterized as *regular,* for which the intensity of the B' peak is proportional to (a) the strength of the absorption due to the B nitrogen component; (b) the strength of the absorption due to the D component; and (c) the strength of the $[N_3V]^0$ optical absorption. Woods[19] proposed that $[N_3V]^0$ centers are formed from minor side reactions occurring during the transformation of $[N\text{-}N]^0$ into B centers.

The room-temperature uv/visible absorption of the sample studied here is shown in Fig. 4. The $[N_3V]^0$ optical absorption between about 3.0 and 3.5 eV is clearly visible. The absorption increases slowly above 3.7 eV, but cannot be correlated with any specific diamond type (i.e., not pure IaA or IaB).

E. ^{14}N ENDOR from the $[N\text{-}C]^0$ and $[N\text{-}N]^+$ centers

^{14}N ENDOR measurements were made on the $[N\text{-}C]^0$ and $[N\text{-}N]^+$ centers by detecting the changes in the dispersion EPR signal at temperatures around 5 K. The enhancement technique described by Newton and Baker[17] was used, and the ENDOR signals were detected using field modulation at 115 KHz, frequency modulation of the radio frequency at 35 Hz and double phase-sensitive detection. Frequency modulation at higher frequencies resulted in smaller ENDOR signals, indicating that the relaxation times governing the ENDOR response are very long. Strong cross-relaxation was observed in the $[N\text{-}N]^+$ and $[N\text{-}C]^0$ ^{14}N ENDOR spectra which complicated the assignment of the transitions.

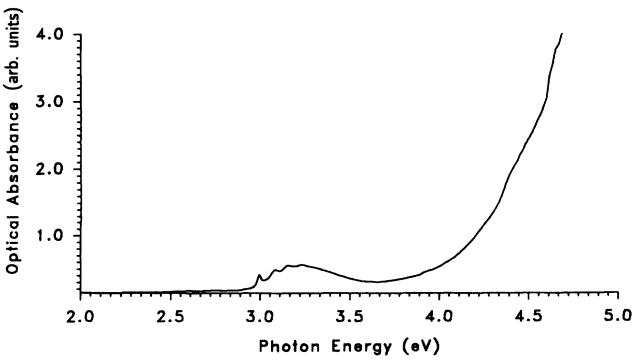

FIG. 4. Visible/ultraviolet absorption spectrum of the diamond studied, measured at 298 K with a slit width of 2 nm.

The ^{14}N ENDOR transitions from the $[N\text{-}N]^+$ center were fitted to the spin Hamiltonian

$$H = g\mu_B \mathbf{S}\cdot\mathbf{B} + \sum_{i=1}^{2} (\mathbf{S}\cdot\underline{\mathbf{A}}_i\cdot\mathbf{I}_i + \mathbf{I}_i\cdot\underline{\mathbf{P}}_i\cdot\mathbf{I}_i - g_N\mu_N\mathbf{I}_i\cdot\mathbf{B}) , \quad (1)$$

where all the terms have their usual meanings. The ^{14}N hyperfine and quadrupole coupling matrices of the two nitrogen nuclei ($i=1,2$) are axially symmetric (identical in magnitude), with the principal axes along $\langle 111 \rangle$ and $\langle \bar{1}\bar{1}\bar{1} \rangle$, respectively. The electronic g value was taken to be 2.0025 (consistent with both our EPR measurements and those of van Wyk and Loubser[11]), and the nuclear g value for both nuclei was taken to be 0.403 760 7, that for a free ^{14}N atom. Only the hyperfine and nuclear quadrupole matrices were varied to optimize the fit to experimental line-position data. The fitting was performed using EPR.FOR,[22] and the parameters determined are given in Table I. The rms difference between observed and calculated ENDOR line positions for the best fit was 27 KHz, which is less than the peak-to-peak linewidth of 85 KHz.

Relaxing the constraints tying the hyperfine (and quadrupole) parameters of the two nuclei to be equal did not improve the quality of the fit. When the nuclear g factors were allowed to vary, they always converged back to the value for free ^{14}N. Nuclear-nuclear interactions ($\mathbf{I}_1\cdot\underline{\mathbf{J}}\cdot\mathbf{I}_2$) between the two nitrogens were considered but appear to be far too small to have any significant effect on the ENDOR transition frequencies. This is unfortunate because a measurement of a purely dipolar nuclear-nuclear interaction could have been used to determine accurately the nitrogen-nitrogen separation.

F. Lifetime of the $[N\text{-}N]^+$ center

Van Wyk and Loubser[11] reported that the lifetime of the $[N\text{-}N]^+$ center at room temperature varies from sample to sample, and ranges from less than a second to many hours. We have made detailed measurements at temperatures between 5 and 50 K, on one sample in which at room temperature the $[N\text{-}N]^+$ disappeared instantaneously when the light was switched off.

In Sec. III B we discussed the desaturating effect of the light and rf enhancement. When the light is switched off, the conditions of saturation change. This effect, com-

TABLE I. ^{14}N hyperfine and quadrupole parameters for $[N\text{-}N]^+$, measured at 5 K.

Ref. 11	Present study
$g = 2.0025 \pm 0.0005$	$g = 2.0025 \pm 0.0005$
$A_\parallel = 154.7(3)$ MHz$\parallel\langle 111 \rangle$	$A_\parallel = 155.26(2)$ MHz$\parallel\langle 111 \rangle$
$A_\perp = 81.0(3)$ MHz	$A_\perp = 81.51(1)$ MHz
	$P_\parallel = -2.245(5)$ MHz$\parallel\langle 111 \rangle$

bined with any sample temperature change, complicates the interpretation of changes in EPR intensity immediately after the light is removed. In an attempt to minimize the change in saturation conditions after the light was switched off, the rf enhancement described in Sec. III B was used to maximize the signal intensity.

Figure 5 shows the dependence of the intensity of one of the EPR lines of the $[N\text{-}N]^+$ center, after the light has been switched off, at temperatures between 6 and 50 K. Great care was taken to stabilize the magnetic field and the EPR spectrometer, so as to ensure that the resonance condition did not vary. At 6 K the $[N\text{-}N]^+$ EPR is easily observable for times longer than 30 min after the light has been switched off. However at 50 K this signal decays away almost entirely within 30 min. When the light is switched off the signal height changes markedly over the first 10–20 sec; both decreases and increases in the signal height can be observed, depending on the temperature. After about 20 sec, the $[N\text{-}N]^+$ center shows a slow and steady decrease in intensity. The long-term decay does not show an exponential dependence in time but (as can be seen in Fig. 5); at low temperatures the $[N\text{-}N]^+$ EPR intensity plotted against the logarithm of time does produce a straight line. In Fig. 5, the EPR signal intensity has been corrected assuming a Curie-law variation with temperature. The rate of decay is approximately temperature independent for measurements below about 20 K.

G. Excitation energy dependence of the $[N\text{-}N]^+$ EPR intensity

Van Wyk and Loubser[11] reported that photons of energy greater than 3.0 eV (415 nm) are necessary to produce the $[N\text{-}N]^+$ center. The dependence of the intensity of the EPR spectra of $[N\text{-}N]^+$ and $[N\text{-}C]^0$ on the energy of the incident photons was studied using the Hg lamp and monochromator. Measurements were made at peaks in the Hg lamp emission and were corrected for the variation in incident intensity. It is clear from the results in Fig. 6 that photons of energy less than 2.3 eV are ineffective for the excitation of $[N\text{-}N]^+$, whereas photons of energy greater than ≈ 2.9 eV create more than an order of magnitude more centers. Increasing the energy above 3.0 eV does not dramatically increase the number of $[N\text{-}N]^+$ centers created. The dependence in the intensity of the $[N\text{-}C]^0$ center on the photon energy is much weaker.

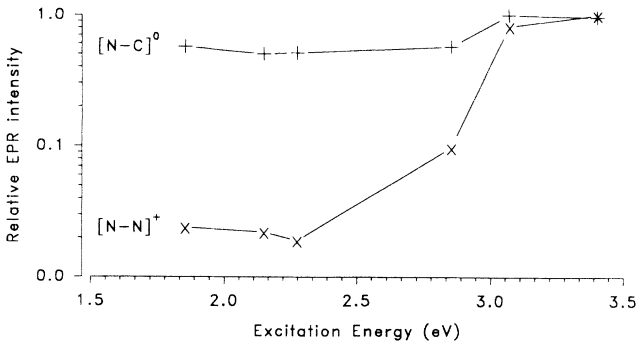

FIG. 6. The $[N\text{-}N]^+$ and $[N\text{-}C]^0$ EPR intensity at 5 K, plotted against the photon energy of the incident radiation.

H. The $[N\text{-}N]^+$ center in powdered diamond

Loubser[23] reported EPR measurements on natural diamond powders, with average particle sizes in the range 0.5 to 30 μm. He suggested that the spectra observed in natural diamond powder, which increased in intensity as the average particle size was decreased, was from the *O*1 center (Erchak *et al.*[24] proposed that *O*1 is a carbon interstitial associated with a vacancy $[C_i + V]$) observed in radiation-damaged diamond. Some of the features of the $[N\text{-}N]^+$, $[N\text{-}C]^0$, and *O*1 powder EPR spectrum occur in approximately the same positions; confusion is possible if not all of the lines of the $[N\text{-}N]^+$ are observed. Loubser noted that the center he had observed in the natural-diamond powder did not follow the annealing behavior of the *O*1 center in single-crystal diamond.

A reexamination of the data presented by Loubser[23] indicates that the center observed in the unirradiated natural diamond power is not *O*1 but is the $[N\text{-}N]^+$ center. To investigate the occurrence of $[N\text{-}N]^+$ in powdered diamond, a fraction of a diamond single-crystal (in which the $[N\text{-}N]^+$ center could only be observed after illumination) was ground into a powder. It was estimated that the average diamond particle size was about 50 μm. EPR of the $[N\text{-}N]^+$ center was then observed without illumination, Fig. 7, and the signal intensity increased on illumination with photons of energy greater than 2.9 eV. To the best of our knowledge the $[N\text{-}N]^+$ center has not been observed in synthetic-diamond powders containing single substitutional nitrogen. However, we speculate that it might be fairly common in powdered natural diamond containing $[N\text{-}N]^0$ centers. Identifying the center observed by Loubser as $[N\text{-}N]^+$ indicates that the intensity of this center in diamond powders correlates with the reciprocal of the particle radius. This implies that a defect created near the surface may be acting as a trap and/or donor of an electron, transforming $[N\text{-}N]^0$ or

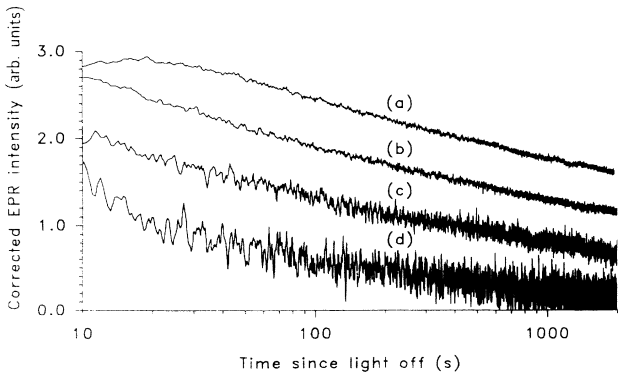

FIG. 5. Change in the EPR intensity of the low-field $(\mathbf{B}\|\langle 100\rangle)^{14}N$ hyperfine line of $[N\text{-}N]^+$, at several temperatures, with the logarithm of time after the light has been switched off. The EPR signal intensity has been corrected for the Curie-law variation with temperature. (a) 6, (b) 10, (c) 27, and (d) 54 K.

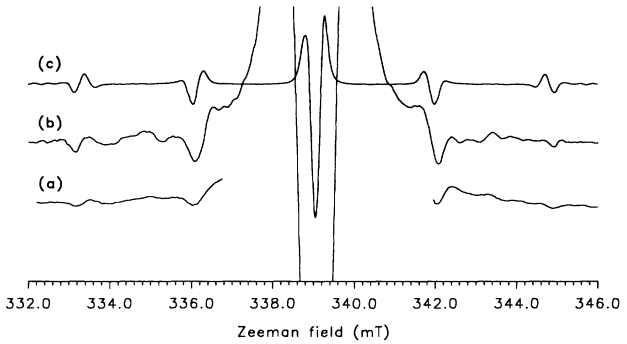

FIG. 7. Second-harmonic 9.65 GHz EPR spectra from powdered Cape Yellow diamond: (a) No illumination, $T=5$ K, (b) With Hg lamp illumination, $T=20$ K, and (c) simulation for the $[N\text{-}N]^+$ center.

$[N\text{-}N]^{2+}$ to the $[N\text{-}N]^+$ center. It is clear that the charge state of the [N-N] center depends on the presence of other defects close to or on the surface of the diamond.

I. The inhomogeneous distribution of $[N\text{-}N]^+$ centers created by illumination

Vay Wyk and Loubser[11] showed that the $[N\text{-}N]^+$ center is not created uniformly through a diamond illuminated from one side. In order to investigate this phenomenon we cut the diamond into two pieces of different thicknesses, but with one face identical so that equal surface areas could be illuminated. The ratio of the masses of the two pieces was 5.051(4), whereas the ratio of the intensity of the $[N\text{-}N]^+$ EPR signals excited by illumination with the full spectrum of the Hg lamp was 3.1(3).

IV. DISCUSSION

A. The unpaired-electron molecular wave function

The unpaired-electron wave function can in general be written as

$$\Phi=\sum_i \eta_i\phi_i \ , \tag{2}$$

where the summation is over the various atoms on which the unpaired-electron probability density is nonzero. For carbon and nitrogen atoms, ϕ_i was constructed from $2s$ and $2p$ hydrogenic orbitals:

$$\phi_i=\alpha_i\psi_{2s}+\beta_i\psi_{2p} \ . \tag{3}$$

The parameters α_i, β_i, η_i, taken to be real, are deduced from the hyperfine parameters in the usual way (e.g., Watkins and Corbett,[25] Morton and Preston[26]). The hybridization ratio is $\lambda_i\equiv\beta_i/\alpha_i$. The fraction of unpaired-electron population in a $2p$ orbital on a nitrogen or carbon atom is $(f_{2p})_i\equiv\eta_i^2\beta_i^2$. We consider the unpaired electron to be in the lowest-energy antibonding orbital σ^* composed of $2s$-$2p$ hybrids [Eq. (3)] on each of the two nitrogen atoms of the $[N\text{-}N]^+$ center, or on the nitrogen and unique carbon atom of the $[N\text{-}C]^0$ center. The parameters for the principal nuclei of $[N\text{-}N]^+$ and $[N\text{-}C]^0$ are given in Table II. This simple one-electron approach (ignoring the overlap of the one-electron wave functions) indicates that for $[N\text{-}C]^0$ approximately 92% of the unpaired-electron population is in the orbital σ^* formed between N and C atoms. For $[N\text{-}N]^+$, approximately 100% of the unpaired-electron population is in the orbital σ^* between the two N atoms. The larger percentage for the $[N\text{-}N]^+$ center may be a consequence of the extra positive charge, compared to the $[N\text{-}C]^0$ center. For the $[N\text{-}C]^0$ center, most of the unpaired-electron population is on the unique carbon neighbor (67% on C and 25% on N, Table II), while for $[N\text{-}N]^+$ the unpaired-electron population is shared equally between the two nitrogens.

The distribution of unpaired-electron population on carbon atoms surrounding $[N\text{-}C]^0$ has been studied by ^{13}C ENDOR.[2] For $[N\text{-}N]^+$ the small isotropic ^{13}C hyperfine interaction [12.3(5) MHz, Sec. III C] was assigned to a ^{13}C atom in one of the two groups of six equivalent nearest neighbors. The anisotropic component of the hyperfine interaction, for a nearest-neighbor ^{13}C (light shading, Fig.2), arising from the dipolar interaction between the unpaired electron in the N-N antibonding orbital and the ^{13}C nucleus, would be expected to be much larger than the uncertainty in the measured hyperfine coupling. However, a very small anisotropic coupling at this site may arise from the cancellation of contributions arising from different mechanisms, as was the case for a N^+ atom in this site in the $[N\text{-}C\text{-}N^+]$ (N1) center.[14] By analogy with the $[N\text{-}C]^0$ center we might expect a ^{13}C atom at one of the six equivalent next-nearest-neighbor sites (medium shading, Fig. 2) to have the largest ^{13}C hyperfine interaction, owing to hyperconjugation. We would expect this to have a greater anisotropy than that measured. With the information available it is difficult to decide between the two different types of six equivalent neighbors. However, the small anisotropy and the small magnitude in the measured ^{13}C interaction indicate negligible delocalization of the unpaired electron onto neighboring carbon atoms, which is consistent with the finding that almost all of the

TABLE II. Hyperfine and quadrupole parameters (measured at 5 K) for $[N\text{-}N]^+$ and $[N\text{-}C]^0$, together with wave function parameters. See text for further details.

		A_s (MHz)	A_p (MHz)	η_1^2	λ_1^2	f_{2p}	$P_\parallel$ (MHz)
$[N\text{-}C]^0$	^{14}N[a]	92.223(2)	10.905(2)	0.247	3.85	0.196	−3.973(1)
	^{13}C[a]	205.744(5)	66.213(5)	0.671	11.32	0.616	
$[N\text{-}N]^+$	^{14}N	106.09(2)	24.58(2)	0.502	7.51	0.443	−2.245(5)

[a]Reference 2.

unpaired electron population exists in the orbital σ^* between the two nitrogen atoms.

B. Determination of bond angles and bond lengths

Recent theoretical studies have considerably enhanced our understanding of several defects in diamond. Work by Briddon, Heggie, and Jones[27] and Kajihara *et al.*[28] on the $[N\text{-}C]^0$ center has shown that (a) for the undistorted substitutional nitrogen center (T_d) there is a singly occupied A_1 state in the band gap, so that the off-center distortion cannot be described by a manifestation of the Jahn-Teller effect and is simply a consequence of the chemical bonding; and (b) the extension of the unique N-C bond is large. The calculated displacements of the unique carbon and of the nitrogen atom are given in Table III. Briddon and co-workers[27,10] have assigned all the observed frequencies to specific vibrational modes.

Briddon and co-workers[27,10] and Jones, Briddon, and Oberg[29] have treated the $[N\text{-}N]^0$ center theoretically. Their calculations show (a) the defect gives a doubly occupied electronic level around midgap, (b) the two nitrogens move towards the planes of their carbon neighbors, giving a N-N separation of 2.14 Å and N-C bonds of 1.46 Å; and (c) the trigonal symmetry of the defect is maintained.

In Fig. 8, we show a defect $[X\text{-}Y]$ incorporated into the diamond lattice. X and Y can be considered to be the nitrogen and unique carbon of the $[N\text{-}C]^0$ center, or the two nitrogens of the $[N\text{-}N]^+$ center. The defect in Fig. 8 has C_{3v} symmetry about the line joining X and Y. To calculate the extension of the X-Y bond relative to the normal C-C bond length, we assume that the six carbon atoms (stippled in Fig. 8) are fixed in the undistorted diamond lattice positions and that the atoms X and Y are allowed to be displaced towards their basal planes (group of three equivalent atoms). Following the discussion of Coulson,[30] we assume that the orthogonality conditions are applicable and valid, such that the angles ω_{mn} between the mth and nth sp-hybridized orbitals on any atom are determined from the condition

$$\lambda_m \lambda_n \cos\omega_{mn} + 1 = 0 , \tag{4}$$

where λ_m, λ_n are the hybridization ratios for these orbitals. The C_{3v} symmetry of the defect, ensures that the angles θ_X (θ_Y) and ϕ_X (ϕ_Y) in Fig. 8 are related by

$$\cos\phi_{X,Y} = (3\cos^2\theta_{X,Y} - 1)/2 . \tag{5}$$

Hence it can be shown from 4 and 5 that θ_X (θ_Y) is given by

$$\cos^2\theta_{X,Y} = \frac{1}{3+2\lambda_{X,Y}^2} , \tag{6}$$

where λ_X (λ_Y) is the hybridization ratio for the unique orbital on atom X (Y). Following simple geometrical considerations the displacement of X or Y towards their basal planes is predicted to be

$$\Delta_{X,Y} = \frac{d}{3}\left[1 - \frac{2}{\sqrt{1+\lambda_{X,Y}^2}}\right] , \tag{7}$$

where d is the undistorted C-C bond length. The hybridization ratios can therefore be used to estimate bond angles and approximate bond extensions.

Edwards and Fowler[31] showed that the approach outlined above, based on directionality and orbital orthogonality, is in striking disagreement with a variety of self-consistent calculations when applied to the E' and P_b centers in SiO_2. They demonstrated that it is not necessary that the molecular orbitals point along bond directions, and that neutral-atom wave functions are not necessarily appropriate when considering defects in partially ionic materials. However, the neutral-atom wave functions have been widely used when analyzing hyperfine coupling constants of defects in diamond and appear to work fairly well. For the defects in diamond considered here it is not obvious why the molecular orbitals should not point along bond directions; after all, the unpaired electron is in a σ^* orbital. We proceed with Eq. (7), bearing in mind the problems outlined by Edwards and Fowler.

The displacements calculated from the EPR data and Eq. (7) for the $[N\text{-}N]^+$ and $[N\text{-}C]^0$ centers are given in

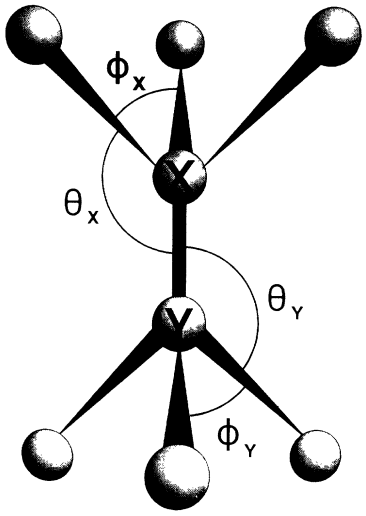

FIG. 8. Model C_{3v} defect used for bond-extension calculation. See text for details.

TABLE III. Calculated displacements (Δ) of the nitrogen and carbon atoms, together with the extension (%) of the unique N-C or N-N bond over the normal C-C bond length for the centers $[N\text{-}C]^0$, $[N\text{-}N]^0$, and $[N\text{-}N]^+$.

	Ref. 10	Ref. 28	Present study
$[N\text{-}C]^0$	C: Δ=0.2 Å	C: Δ=0.22 Å	^{13}C: Δ=0.22 Å
	N: Δ=0.2 Å	N: Δ=0.17 Å	^{14}N: Δ=0.05 Å
	Extension ≈28%	Extension ≈25%	Extension ≈20%
$[N\text{-}N]^0$	N: Δ=0.3 Å		
	Extension ≈40%		
$[N\text{-}N]^+$			^{14}N: Δ=0.16 Å
			Extension ≈21%

Table III, which also contains displacements predicted by recent *ab initio* calculations on the $[N\text{-}C]^0$ and $[N\text{-}N]^0$ centers. For $[N\text{-}C]^0$, the N-C bond extension determined by Eq. (7) is of the same order as that calculated by Briddon and Jones[10] and by Kajihara *et al.*[28] However, Eq. (7) predicts a marked anisotropy in the relative displacements of the nitrogen and unique carbon atom. The smaller displacement predicted for the nitrogen may result from the inadequacies of the approach, or it may indicate that the N-C bonds are stronger than the C-C bonds. Equation (7) suggests that the N-N extension for the $[N\text{-}N]^+$ center is approximately the same as for the $[N\text{-}C]^0$ center. Intuition suggests that this is reasonable, if the bond extension is primarily influenced by placing an electron in the antibonding orbital. The symmetric displacement of both nitrogens is consistent with the equal strength of all of the N-C bonds. We note that the 21% extension of N-N bond in the $[N\text{-}N]^+$ is much smaller than that predicted for $[N\text{-}N]^0$, suggesting that accommodating a second electron in the antibonding orbital requires considerable lengthening of the bond.

Equation (7) predicts intuitively consistent results for the $[N\text{-}C]^0$ and $[N\text{-}N]^+$ centers, and is in qualitative accord with more sophisticated calculations.[26–28] It is of course possible that the agreement for $[N\text{-}C]^0$ is fortuitous, confirmation of the result for $[N\text{-}N]^+$ with a more refined theoretical approach would be very useful.

C. The ^{14}N quadrupole interaction

^{14}N ENDOR measurements accurately determine the nuclear quadrupole interaction parameters. The nuclear electric-quadrupole coupling arises from the interaction between the nuclear quadrupole moment, and the electric-field gradient at the nucleus. The quadrupole coupling matrices of the $^{14}N^+$ atoms in the $[N_1\text{-}C\text{-}C\text{-}N_2^+]$ (*W7*) (Ref. 32) and $[N_1\text{-}C\text{-}N_2^+]$ (*N1*) (Ref. 14) centers have been used to infer the environment of this atom. Here we specifically consider substitutional nitrogen in defects, where the nitrogen is trigonally coordinated. The interaction parameters $P_\parallel$ is given by

$$P_\parallel = \frac{3eQV_{zz}}{4I(2I-1)} , \tag{8}$$

where I is the nuclear spin, eQ the nuclear electric quadrupole moment, and V_{zz} the gradient of the electric field at the nucleus. The electric-field gradient receives its greatest contribution from electrons in orbitals on the central atom itself but (unlike the hyperfine interaction) arises from the total electron density, rather than from only the unpaired-electron density.

In Fig. 9 we plot $P_\parallel$ measured for the nitrogen atoms of the $[NV]^-$ (*W15*),[33] $[N\text{-}C]^0$ and $[N\text{-}N]^+$ centers and for N_1 of the $[N_1\text{-}C\text{-}C\text{-}N_2^+]$ (*W7*) and $[N_1\text{-}C\text{-}N_2^+]$ centers, against the fraction of unpaired-electron population (f_{2p}) in a $2p$ orbital on the nitrogen atom. As the nitrogen vacancy center $[NV]^-$ is observed in a $S=1$ state, it must contain an even number of electrons. Hence we assume that it has captured an electron and is in a negative charge state. The correlation between f_{2p} and $P_\parallel$ is surprising, as only unpaired-electron density is considered. The correlation operates over a wide range, from almost pure lone pair $f_{2p}\approx 0$ on the nitrogen, in $[NV]^-$, to $f_{2p}\approx 0.5$ in $[N\text{-}N]^+$, and suggests that f_{2p} is linearly related to the electric-field gradient at the nitrogen nucleus. To proceed further we need to consider carefully the nuclear quadrupole interaction in ^{14}N.

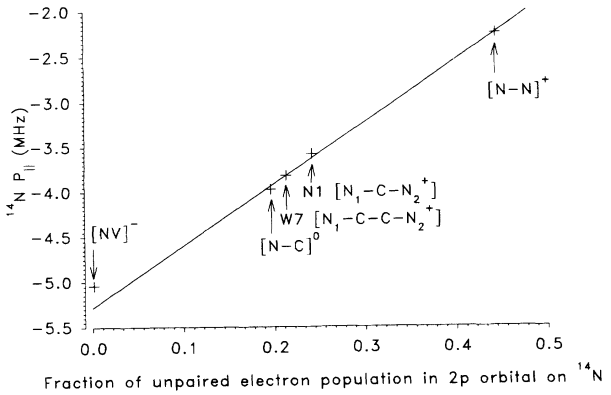

FIG. 9. The fraction (f_{2p}) of the unpaired-electron population in a $2p$ orbital directed along the trigonal symmetry axis for a substitutional nitrogen atom in the specified defects, plotted against the measured ^{14}N quadrupole parameters $P_\parallel$ (MHz). The straight line is a fit to the data shown excluding the lowest plotted point ($[N_3V]^0$) because of the large uncertainty in f_{2p} for this defect.

Several authors[34–36] have calculated values for the electric-field gradient at the nitrogen nucleus of the single substitutional nitrogen defect $[N\text{-}C]^0$. Here we outline a simple calculation which demonstrates some of the physics underlying the measured quadrupole couplings for a number of nitrogen defects in diamond. We construct orbitals on a nitrogen or carbon atom, from $2s$ (ψ_{2s}) and $2p$ (ψ_{2p}) atomic wave functions, while assuming that the atom has undergone a trigonal distortion, so that one unique orbital (ϕ_1) points along the z axis, and three equivalent orbitals (ϕ_2,ϕ_3,ϕ_4) all make the same angle with the z axis. In the crystal, molecular orbitals are formed as a linear combination of these atomic orbitals on each atom. For the jth N-X bond (where X may be N or C) the bonding and antibonding orbitals are

$$\begin{aligned}\Phi_{jB} &= |\eta_{jB}^{N}|\phi_j^{N} + |\eta_{jB}^{X}|\phi_j^{X} + \cdots ,\\ \Phi_{jA} &= |\eta_{jA}^{N}|\phi_j^{N} - |\eta_{jA}^{X}|\phi_j^{X} + \cdots ,\end{aligned} \tag{9}$$

where the dots indicate admixtures from other orbitals. To a first approximation we can ignore small admixtures from other atoms and consider only the orbitals of the two atoms between which the occupied antibonding orbital is formed. For the molecular orbital containing the unpaired electron, the measured hyperfine parameters determine $|\eta_{jA}^{N}|$ and $|\eta_{jA}^{X}|$. The values of $|\eta_{jB}^{N}|$ and $|\eta_{jB}^{X}|$ may be calculated if the overlap integral $\langle\phi_j^{N}|\phi_j^{X}\rangle$ is known. For a normal C-C bond, the overlap integral is about 0.4,[34] but for an elongated bond containing an extra electron, $\langle\phi_1^{N}|\phi_1^{X}\rangle$ is probably very much less than 0.4. The values of $|\eta_{jA}^{N}|$ and $|\eta_{jA}^{C}|$ for the $[N\text{-}C]^0$ and $[N\text{-}N]^+$ centers given in Table II imply that $\langle\phi_1^{N}|\phi_1^{X}\rangle\approx 0$,

since $|\eta_{1A}^{N}|^2+|\eta_{1A}^{C}|^2$ ([N-C]^0) and $|\eta_{1A}^{N}|^2+|\eta_{1A}^{N}|^2$ ([N-N]$^+$) are approximately equal to 1.

Assuming that only electrons in orbitals on the nitrogen contribute the electric-field gradient may be expressed as

$$V_{zz}=-|e|[2|\eta_{1B}^{N}|^2+|\eta_{1A}^{N}|^2]\left\langle\phi_1\left|\frac{3\cos^2\theta-1}{r^3}\right|\phi_1\right\rangle -2|e|\sum_{j=2}^{4}|\eta_{jB}^{N}|^2\left\langle\phi_j\left|\frac{3\cos^2\theta-1}{r^3}\right|\phi_j\right\rangle , \quad (10)$$

where θ is the angle between the z axis and the radial vector r, e is the electron charge, and the factors of 2 multiplying $|\eta_{1B}|^2$ are there because there are two electrons in each bonding orbital. Performing this summation over the orbitals gives

$$V_{zz}=\frac{4|e|\lambda_1^2}{15(1+\lambda_1^2)}\langle r_{2p}^{-3}\rangle[-2|\eta_{1B}^{N}|^2-|\eta_{1A}^{N}|^2+2|\eta_{2B}^{N}|^2] , \quad (11)$$

where λ_1 is the hybridization ratio for ϕ_1 (see Table II). In this expression we have taken $|\eta_{2B}^{N}|=|\eta_{3B}^{N}|=|\eta_{4B}^{N}|$. The first two terms in the square bracket are determined from the hyperfine parameters, but we do not know $|\eta_{2B}^{N}|^2$. The extra positive charge on the nitrogen atom may make $|\eta_{2B}^{N}|^2>|\eta_{2B}^{C}|^2$, but the large value of $\langle\phi_2^{N}|\phi_2^{C}\rangle$ (probably about 0.4) will reduce both. However, the large value of $\langle\phi_2^{N}|\phi_2^{C}\rangle$ also makes it invalid to consider only ϕ_2^{N} as contributing to V_{zz} since the overlap region with high electron density will increase the contribution of these back bonds. From Eqs. (8) and (11) we obtain

$$P_{\parallel}=\frac{P_0\lambda_1^2}{1+\lambda_1^2}[-2|\eta_{1B}^{N}|^2-|\eta_{1A}^{N}|^2+2|\eta_{2B}^{N}|^2] , \quad (12)$$

where $P_0=-[e^2Q/5I(2I-1)]\langle r_{2p}^{-3}\rangle$, the quadrupole interaction parameter for a single electron in a pure $2p_z$ orbital. The values of $P_{\parallel}$, $\lambda_1^2/(1+\lambda_1^2)$, and $|\eta_{1A}|^2$ are determined from experiments. If we assume that $\langle\phi_1^{N}|\phi_1^{X}\rangle\approx 0$, then constraining the orbitals in Eq. (9) to be orthogonal and normalized leads to $|\eta_{1B}^{N}|^2\approx 1-|\eta_{1A}^{N}|^2$ and

$$P_{\parallel}=-P_0f_{2p}+\frac{2P_0\lambda_1^2}{1+\lambda_1^2}[1-|\eta_{2B}^{N}|^2] . \quad (13)$$

The experimental data in Fig. 9 indicate that the measured quadrupole interaction is proportional to f_{2p}, which is consistent with Eq. (13) so long as the second term is constant over the defects considered. The linear relation in Fig. 9 implies that $P_0=-6.7(3)$MHz. This is in excellent agreement with the value of $P_0=-6.75$ MHz quoted as standard for nitrogen.[37] Considering the second term in Eq. (13) we see that in order for it to remain constant a small increase in $\lambda_1^2(1+\lambda_1^2)$ must be accompanied by an increase in $|\eta_{2B}^{N}|^2$. We note that for [N-N]$^+$ $\lambda_1^2/(1+\lambda_1^2)$ is 0.88 and for [NV]$^-$ it is 0.5, for the other defects it is close to 0.8. For [NV]$^-$ there is a large uncertainty in $\lambda_1^2/(1+\lambda_1^2)$ because the small anisotropic hyperfine coupling is not well determined. Hence Eq. (13) indicates a relative stability in the value of $|\eta_{2B}^{N}|^2$. From the intercept in Fig. 9 we deduce that $|\eta_{2B}^{N}|^2\approx 0.5$, which is reasonable.

Once the quadrupole interaction is known, f_{2p} can be estimated using Eq. (13). We note that, for the [NV]$^-$ center, Eq. (13) implies $f_{2p}=0.02$, which is an order of magnitude greater than determined in the usual way from the nitrogen hyperfine parameters.[33] Because of all the possible contributions to the nitrogen hyperfine interaction (distant dipolar, spin polarization, etc.) which were not taken into account in the calculation of f_{2p} from the hyperfine parameters, we postulate that the value 0.02 determined from the quadrupole interaction is more realistic.

D. The various ionization states of the [N-N] species

It has been assumed that the usual charge state of the A center is neutral, i.e., [N-N]^0. Since here the lowest energy N-N antibonding orbital is already full, a [N-N]$^-$ center with trigonal symmetry is not expected to be formed.

Van Wyk and Loubser[11] commented that [N-N]$^+$ could be created by ionization of [N-N], or via electron capture by [N-N]$^{2+}$. In the sample studied here, the concentration of [N-N]^0 centers is two orders of magnitude greater than the maximum concentration of [N-N]$^+$ centers we can produce by optical excitation. Thus either we are ionizing only a very small fraction, limited perhaps by the number of suitable electron traps, or the [N-N]$^+$ centers observed are being produced by electron capture by [N-N]$^{2+}$, which is present in much lower abundance than that of [N-N]^0. (The infrared absorption can be successfully fitted without including any unusual features; therefore the concentrations of [N-N]$^+$ and [N-N]$^{2+}$ must be lower than that of [N-N]^0, since presumably they would have different characteristic one-phonon infrared absorptions). If [N-N]$^{2+}$ is present, what acceptor has soaked up the liberated electrons? It would presumably be a very powerful electron trap, and it is not clear why this would be stable when [N-C]^0, which is known to act as a donor, is present. On the other hand, in wide-band-gap materials like diamond, one cannot be sure that the Fermi level is well defined, so that species may well exist in unexpected charge states.

The [N-N]^0 center produces an optical absorption line at 3.8 eV.[8] In IaA diamonds a secondary absorption edge at this energy is clearly visible. Production of the [N-N]$^+$ center by light of energy appreciably less than 3.8 eV indicates that the process is not simply ionization of the [N-N]^0 center. The increase in the production of [N-N]$^+$ with excitation energy (Fig. 6) correlates with the onset optical absorption of the [N_3V]^0 center (Fig. 4), which suggests that this center may be involved with its production. No clear change in the [N_3V]^0 EPR intensity was observed when creating [N-N]$^+$ however, any change in one of the [N_3V]^0 EPR lines would have been very small, because of the large number of lines, and the much higher concentration of [N_3V]^0. Therefore, it is not possible to rule out direct charge transfer from [N_3V]^0 to [N-N]$^{2+}$ creating [N_3V]$^+$ and [N-N]$^+$.

The results presented in Sec. III F, showing the decay in the number $[N\text{-}N]^+$ with time when the light is switched off, are reminiscent of those obtained for the photochroism of the H2 and H3 centers in diamond.[38] The H2 center ($[N\text{-}V\text{-}N]^-$) is the negative charge state of the H3 ($[N\text{-}V\text{-}N]^0$) center. The decay of the $[N\text{-}N]^+$ EPR intensity with the logarithm of time suggests that there is a wide distribution of lifetimes of the $[N\text{-}N]^+$ centers created, presumably resulting from a large variation in the separation between the $[N\text{-}N]^+$ center and its electron donor and/or trap. Below about 20 K, the decay rate is independent of temperature, indicating tunneling between the donor and/or trap and the $[N\text{-}N]^+$ center; at higher temperatures, thermally actived hopping also contributes. Although our measurements show that the $[N\text{-}C]^0$ and $[N_3V]^0$ EPR intensities also decrease slightly when the exciting light was switched off, it was not possible to identify a one-to-one charge-transfer process between any of the defects studied. However, $[N\text{-}C]^0$ and $[N_3V]^0$ may be two of the donors and/or traps involved in the creation and subsequent decay of the $[N\text{-}N]^+$ center.

It is a very interesting result (in Sec. III G) that, in finely divided diamond, $[N\text{-}N]^+$ can exist in equilibrium with $[N\text{-}N]^0$ whereas, in the single crystal, it was only observed after illumination. This means that a defect created near the surface is acting as a trap and/or donor of an electron, transforming $[N\text{-}N]^0$ or $[N\text{-}N]^{2+}$ to the $[N\text{-}N]^+$ center. We presume that $[N\text{-}N]^+$ centers themselves are not to be found at the surface; the strained and irregular environment near the surface would give rise to a spread in the measured hyperfine and quadrupole parameters of the nitrogens, which is not observed. We have no information that allows us to determine the nature of the trap and/or donor, nor do we know the average $[N\text{-}N]^0$ or $[N\text{-}N]^{2+}$ trap and/or donor separation. We do know that when diamond is crushed, an isotropic resonance at $g=2.0027(2)$ and linewidth of about 0.55 mT is created,[39] which is attributed to defects near the surface. Strong absorption around $g=2.0$, due to $[N_3V]^0$ and other centers, precludes study of this defect in the sample used in our study. The number of $[N\text{-}N]^+$ centers was increased by illumination (Fig. 7) indicating that not all the potential $[N\text{-}N]^+$ centers were activated by surface traps and/or donors.

In Sec. III I it was confirmed that the $[N\text{-}N]^+$ centers are not created uniformly through a diamond when illuminated from one side. Assuming that the number of centers produced at a distance x into the diamond falls off as $\exp(-kx)$, one can calculate from the data in Sec. III I that $k \approx 0.7\ \text{mm}^{-1}$, which is less than, but of the order of, the optical-absorption coefficient of the $[N_3V]^0$ center at 2.985 eV. It appears that excitation of this center plays a role in the creation of $[N\text{-}N]^+$.

In summary, from the information available we cannot determine whether $[N\text{-}N]^+$ is created by ionization of $[N\text{-}N]^0$ or electron capture by $[N\text{-}N]^{2+}$. If it is the latter, then the equilibrium concentration of $[N\text{-}N]^{2+}$ in the sample studied here need only be 1% of the $[N\text{-}N]^0$ concentration. The study of the powdered diamond is significant because it indicates that, given the right traps and/or donors, $[N\text{-}N]^0$, $[N\text{-}N]^+$, and possibly $[N\text{-}N]^{2+}$ can all be present at the same time. The observation of different charge states of the same defect ($[N\text{-}C]^0$ and $[N\text{-}C]^+$, $[V]$ and $[V]^-$, $[N\text{-}V\text{-}N]$ and $[N\text{-}V\text{-}N]^-$) is becoming a common occurrence in diamond.

V. CONCLUSION

There can be no doubt that the *W*24 center is $[N\text{-}N]^+$. For $[N\text{-}N]^+$, the hyperfine and quadrupole interactions show that both nitrogens are equivalent. In single-crystal diamond containing $[N\text{-}N]^0$ and $[N_3V]^0$ centers, $[N\text{-}N]^+$ is created by excitation with light of energy greater than 3.0 eV. We have not been able to identify the electron trap(s) or donor(s) associated with the $[N\text{-}N]^+$ center. It is clear that $[N\text{-}N]^+$ is not created homogeneously throughout the diamond, but occurs close to the surface receiving the illumination. The rate of decay of $[N\text{-}N]^+$ after the exciting light is removed is sample dependent. However, for one sample studied in detail, it was shown that (a) at sufficiently low temperature the number of centers remaining after the excitation is switched off varies linearly with the logarithm of time, indicating a wide distribution in the trap and/or $[N\text{-}N]^+$ center separation; (b) the decay rate is temperature independent at low temperatures, indicating tunneling between the trap and $[N\text{-}N]^+$ center; and (c) at higher temperatures, thermally activated hopping contributes to the decay of $[N\text{-}N]^+$ centers. When a single crystal diamond, in which the $[N\text{-}N]^+$ center is only observed upon illumination, is crushed to a powdered form, the $[N\text{-}N]^+$ center is observed without illumination. This suggests that defects at (or close to) the surface act as traps, converting $[N\text{-}N]^0$ to $[N\text{-}N]^+$.

A simple calculation of bond lengths from the hyperfine parameters suggests that the N-C bond length in the $[N\text{-}C]^0$ center is very similar to the N-N bond length in the $[N\text{-}N]^+$ center. The quadrupole interaction for the substitutional nitrogen atoms of the $[N\text{-}N]^+$ center is consistent with those measured in other nitrogen defects in diamond, and is explained remarkably well by as simple model. It is clear for the defects considered here that the magnitude of the quadrupole interaction is directly related to the fraction of unpaired-electron population in a $2p$ orbital on a substitutional nitrogen atom.

ACKNOWLEDGMENTS

We acknowledge the guidance and encouragement we received from the late Professor J. H. N. Loubser. O.D.T. thanks De Beers Industrial Diamond Division for financial support. We thank Dr. R. J. Caveney and his associates at the Diamond Research Laboratory, Johannesburg, for provision of samples and their continued interest in the research program. We acknowledge the help of Dr. C. Welbourn, and his colleagues at the Diamond Trading Company, Research Laboratory, Maidenhead, with sample preparation, and R. Hall of De Beers Industrial Diamond Division (Ireland) for arranging the powdering of the diamond. We thank Professor J. A. Weil for the simulation and fitting software EPR.FOR, and the Department of Physics, Oxford, for partial financial support.

*Author to whom correspondence should be addressed.
[1]W. V. Smith, P. P. Sorokin, I. L. Gelles, and G. J. Lasher, Phys. Rev. **115**, 1546 (1959).
[2]A. Cox, M. E. Newton, and J. M. Baker, J. Phys. Condens. Matter **6**, 551 (1994).
[3]A. Cox, Ph.D. thesis, University of Oxford, 1993.
[4]R. M. Chrenko, R. E. Tuft, and H. M. Strong, Nature (London) **270**, 141 (1977).
[5]A. T. Collins, J. Phys. C **13**, 2641 (1980).
[6]T. Evans and Z. Qi, Proc. R. Soc. London Ser. A **381**, 159 (1982).
[7]T. Evans, in *The Properties of Natural and Synthetic Diamond,* edited by J. E. Field (Academic, London, 1992).
[8]G. Davies, J. Phys. C **9**, L537 (1976).
[9]G. B. B. M. Sutherland, D. E. Blackwell, and W. G. Simeral, Nature (London) **174**,901 (1954).
[10]P. R. Briddon and R. Jones, Physica B **185**, 179 (1993).
[11]J. A. van Wyk and J. H. N. Loubser, J. Phys. C **16**, 1501 (1983).
[12]J. A. Van Wyk and J. H. N. Loubser, J. Phys. Condens. Matter **5**, 3019 (1993).
[13]J. A. van Wyk, J. H. N. Loubser, M. E. Newton, and J. M. Baker, J. Phys. Condens. Matter **4**, 2651 (1992).
[14]A. Cox, M. E. Newton, and J. M. Baker, J. Phys. Condens. Matter **4**, 8119 (1992).
[15]J. H. N. Loubser, J. A. van Wyk, and C. M. Welbourn, J. Phys. C **15**, 6031 (1982).
[16]G. Feher and E. A. Gere, Phys. Rev. **114**, 1245 (1959).
[17]M. E. Newton and J. M. Baker, J. Phys. Condens. Matter **3**, 3605 (1991).
[18]C. D. Clark and S. T. Davey, J. Phys. C **17**, 1127 (1984).
[19]G. S. Woods, Proc. R. Soc. London Ser. A **407**, 219 (1986).
[20]G. S. Woods, G. C. Purser, A. S. S. Mtimkulu, and A. T. Collins, J. Phys. Chem. Solids **51**, 1191 (1990).
[21]G. S. Woods, J.A. van Wyk, and A. T. Collins, Philos. Mag. B **62**, 589 (1990).
[22]EPR.FOR (version 5.13); D. G. McGavin, M. J. Mombourquette, and J. A. Weil. Inquiries should be made to Professor J. A. Weil, Department of Chemistry, University of Saskatchewan Saskatoon, SK, S7N 0W0, Canada. Email WEIL@SASK.USASK.CA.
[23]J. H. N. Loubser, Solid State Commun. **22**, 767 (1977).
[24]D. P. Erchak, R. B. Gelfand, N. M. Penina, V. F. Stelmakh, V. P. Tolstykh, A. G. Ulyashin, V. S. Varichenko, and A. M. Zaitsev, Phys. Status Solidi A **121**, 63 (1990).
[25]G. D. Watkins and J. W. Corbett, Phys. Rev. **121**, 1546 (1961).
[26]J. R. Morton and K. F. Preston, J. Magn. Reson. **30**, 577 (1978).
[27]P. R. Briddon, M. I. Heggie, and R. Jones, in *New Diamond Science and Technology 1991,* edited by R. Messier, T. J. Glass, J. E. Butler, and R. Roy, MRS Symposia Int. Proceedings No. NDST2-C3 (Materials Research Society, Pittsburgh, 1991), p. 63.
[28]S. A. Kajihara, A. Antonelli, J. Bernholc, and R. Car, Phys. Rev. Lett. **66**, 2010 (1991).
[29]R. Jones, P. R. Briddon, and S. Oberg, Philos. Mag. Lett. **66**, 67 (1992).
[30]C. A. Coulson, *Valence* (Oxford University Press, Oxford, 1960), p. 187.
[31]A. H. Edwards and W. B. Fowler, Phys. Rev. B **41**, 10 816 (1990).
[32]M. E. Newton and J. M. Baker, J. Phys. Condens. Matter **3**, 3591 (1991).
[33]Xing-Fei He, N. B. Manson, and P. T. H. Fisk, Phys. Rev. B **47**, 8809 (1993); **47**, 8816 (1993).
[34]A. G. Every and D. S. Schonland, Solid State Commun. **3**, 205 (1965).
[35]R. P. Messmer and G. D. Watkins, Phys. Rev. B **7**, 2568 (1973).
[36]N. Sahoo, K. C. Mishra, M. van Rossum, and T. P. Das, Hyperfine Interact. **35**, 701 (1987).
[37]D. T. Edmonds, M. J. Hunt, and A. L. Mackay, J. Magn. Reson. **9**, 66 (1972).
[38]Y. Mita, Y. Ohno, Y. Adachi, H. Kanehara, Y. Nisida, and T. Nakashima, J. Phys. Condens. Matter **2**, 768 (1993).
[39]G. K. Walters and T. L. Estle, J. Appl. Phys. **32**, 1854 (1961).

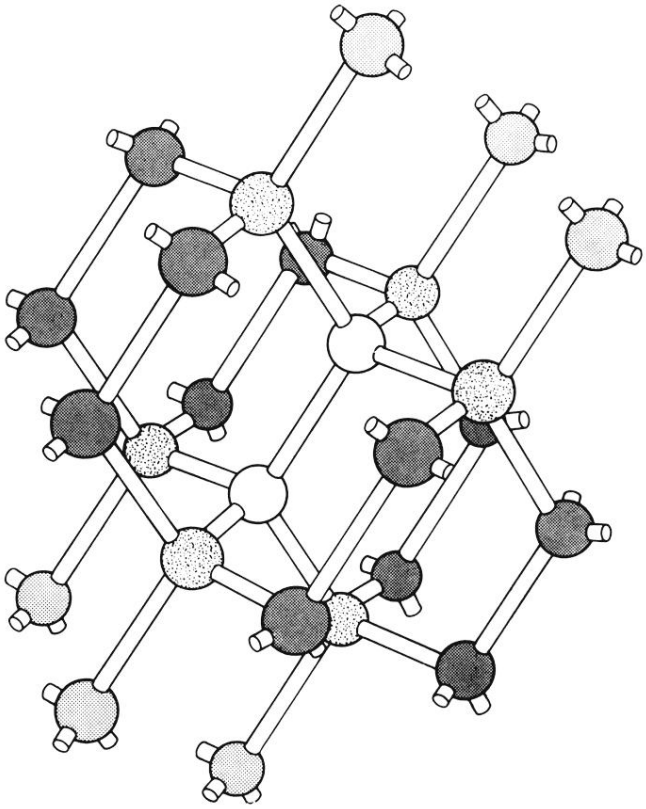

FIG. 2. $[N\text{-}N]^+$ defect in diamond lattice. The two nitrogen atoms are shown unshaded, and the various groups of carbon neighbors are distinguishable by their shading. See text for further details.

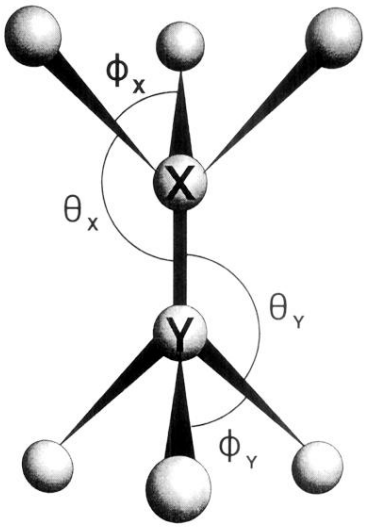

FIG. 8. Model C_{3v} defect used for bond-extension calculation. See text for details.